Low-Band-Shifted Hierarchical Backward Motion Estimation and Compensation for Wavelet-Based Video Coding

Yufei Yuan and Mrinal K. Mandal
Department of Electrical and Computer Engineering
University of Alberta, Edmonton, Alberta, Canada T6G 2V4
E-mail: {yuan, mandal}@ee.ualberta.ca

Abstract

A new framework for block-based backward motion compensation in wavelet scalable video coding scheme is proposed. Motion estimation and compensation are hierarchically conducted in wavelet domain using coarser level lowpass subband in the current frame and synthesized next finer level lowpass subband in the reference frame, hence, the motion information does not need to be transmitted. To alleviate the aliasing effect caused by decimation in wavelet decomposition, the lowpass subband in reference frame are shifted to obtain four subbands, which are then used in motion estimation and compensation to generate final prediction. A flexible quantization scheme and arithmetic coding is used to individually encode the motion compensated subbands without exploiting cross-band correlation. Compared to the motion estimation and compensation scheme without shifting of the lowpass subband, the proposed technique provides around 2 dB improvement in PSNR for compression of full motion sequence. The multi-level scalability of the scheme makes it useful for low bandwidth networks, such as satellite or cellular networks.

1. Introduction

The discrete wavelet transform (DWT) as a powerful signal processing tool has found its application in many research areas. Still image compression is one of the most successful applications in which the DWT has been applied. Because of DWT's outstanding approximation of spatial-spectral density of natural images and its natural support for scalability, the new generation of still image compression standard [4] has moved away from conventional discrete cosine transform (DCT) and adopted DWT as the spatial energy compaction tool. Because DWT outperforms DCT in the compression of still images, it is natural that researchers are interested in building new video compression schemes that is also based on DWT.

In the current video compression standards, motion estimation (ME) and motion compensation (MC) are employed in video codecs to remove the temporal redundancy existed between neighboring video frames. As the DWT decomposes the video frame into a multi-level pyramid composed of subbands in multiple resolutions, it is desirable that ME/MC can be conducted directly on these subbands. However, as shown in [2, 11], the aliasing caused by decimation in wavelet decomposition makes it impossible to do direct band-to-band ME between highpass subbands in neighboring video frames. To avoid the aliasing effect caused by decimation, unsubsampled lowpass subbands have been proposed to be used for ME in wavelet domain.

There are two main categories of schemes for ME in wavelet domain: forward-acting and backward-acting schemes. Meyer *et al* [9] proposed a forward hierarchical ME scheme which is based on a new decomposition structure. In their proposed scheme, the highpass subbands do not undergo decimation procedure. Thus, the motion vectors obtained from ME using lowpass subbands can be directly applied to the highpass subbands without aliasing. The authors argue that encoding of undecimated highpass subbands will not pose serious problem because most of the coefficients in highpass subbands will be quantized to zero. Skowronski [15] proposed to use *algorithme à trous* to generate undecimated subbands and conduct forward pel-recursive ME on subbands. Nosratinia and Orchard [11] were the first to propose a wavelet-based purely backward ME/MC framework, in which motion vectors are estimated both at the encoder and the decoder side using already reconstructed subbands from coarse resolution (higher level) to fine resolution (lower level). Later, Yang and Ramchandran [17] proposed to use upsampled and filtered coarse reference subband to predict current subband at each level. They focused their efforts on the design of an interpolation filter which can alleviate the aliasing effect. Most recently, Lundmark *et al* [8] incorporated motion vector certainty into the backward MC framework to reduce bitrate.

In this paper, we present a new ME/MC scheme which significantly improves the performance of backward block-matching ME in wavelet subbands. The major contribution of our current research lies in exploiting the information available to the decoder to improve the performance of backward ME/MC scheme. Our preliminary experimental results show that the PSNR of reconstructed video frame enjoys an improvement of around 2 dB with the application of the low-band-shifting (LBS) technique.

The paper is organized as follows. We discuss the hierarchical backward ME in Section 2. The proposed low-band-shifted backward ME/MC scheme is presented in Section 3. In Section 4, we describe an implementation of quantization scheme for the encoding of residual subbands. Simulation results are given in Section 5. Section 6 contains the concluding remarks.

2. Hierarchical backward motion estimation/compensation

Fig. 1 illustrates a two-level wavelet decomposition of an image. In order to perform hierarchical backward ME, the lowpass subband at the coarsest resolution of the wavelet pyramid is obtained first. Taking Fig. 1 as an example, we assume that LL_2 is already known to the decoder before ME. To demonstrate the procedure of ME/MC, we use k as time index. Let $LL_{k-1,2}$ denote the second level lowpass subband of the reference frame and $LL_{k,2}$ denote the lowpass subband of the current frame at the same level. We use the following equation to denote the ME between two subbands:

$$MV_{k,n} = ME(LL_{k-1,n}, LL_{k,n}) \qquad (1)$$

where MV denotes motion vectors.

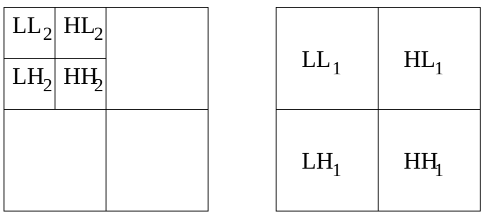

Figure 1: The two-level wavelet decomposition and the subband naming convention.

Because of the aliasing effect, we cannot directly apply $MV_{k,2}$ to the highpass subbands at Level 2 in Frame $k-1$ to obtain the predicted high subbands in Frame k at the same level, which are denoted as $\overline{HL}_{k,2}$, $\overline{LH}_{k,2}$, and $\overline{HH}_{k,2}$. Instead, both $LL_{k-1,2}$ and $LL_{k,2}$ are upsampled and filtered to generate two new subbands $LL^{\uparrow}_{k-1,2}$ and $LL^{\uparrow}_{k,2}$, which have the same size with LL_1 and serve as approximations of $LL_{k-1,1}$ and $LL_{k,1}$. ME is conducted between $LL^{\uparrow}_{k-1,2}$ and $LL^{\uparrow}_{k,2}$. The resulted motion vectors are applied to $LL_{k-1,1}$ to obtain a predicted subband $\overline{LL}_{k,1}$. Then, $\overline{LL}_{k,1}$ is decomposed by one level to generate four subbands, the three highpass subbands serve as the prediction for $HL_{k,2}$, $LH_{k,2}$ and $HH_{k,2}$. The prediction error, *i.e.*, displaced subband difference (DSD), is then quantized and entropy coded. Fig. 2 illustrates the ME scheme proposed in [17]. For simplicity, only one-dimensional processing is shown while the input signal itself is two-dimensional.

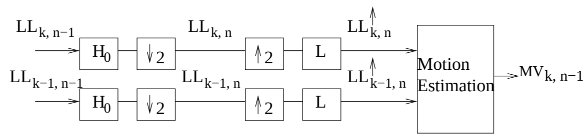

Figure 2: Block diagram for one-level ME. H_0 is the lowpass analysis filter. L is the lowpass interpolation filter. Note that for simplicity, only one-dimensional filtering, decimation, and interpolation are shown.

3. New low band shifting based scheme

Although purely backward ME/MC scheme is achieved in [11, 17], Fig. 3 shows that the scheme illustrated in Fig. 2 cannot estimate the shifting of the signal. Here, the usage of block-matching algorithm (BMA) is assumed. From Fig. 3, we can see that the aforementioned scheme can only estimate the shifting of the signal by even pixels. Another observation is that although the whole reconstructed reference frame is available to the decoder, the aforementioned scheme only uses the LL subband at coarser level to generate an upscaled subband for ME at the neighboring finer level. There may exist a better way to utilize the information available to the decoder.

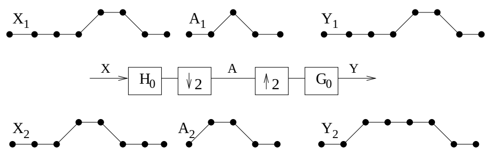

Figure 3: Examples of the coefficients from *Haar* wavelet for a 1-D signal $X_1[n]$ and its shifted-by-one-pixel equivalent $X_2[n]$. H_0 is the lowpass analysis filter and G_0 is the lowpass synthesis filter. The amplitudes of the coefficients are not exactly as shown. Here, we are more interested in the shape of the output signal.

It is fairly straightforward to notice in Fig. 3 that we can still predict $X_2[n]$ if we shift $X_1[n]$ by 1 pixel before conducting ME. This is the basic concept behind the so-called *LBS method*, which is proposed by Park and Kim in [12] to deal with the shift-variant property of wavelet decomposition. However, the authors constructed a new data structure, *i.e.*, wavelet block, to conduct forward ME, which in itself is not hierarchical.

It is observed in Fig. 3 that the reference signal $X_1[n]$ and the approximation of the current signal $X_2[n]$, namely, $A_2[n]$ are available to decoder before ME. What we need is to shift $X_1[n]$ by 1 pixel to generate $X_1^s[n]$, which will be filtered and decimated to generate $A_1^s[n]$. Both $A_1[n]$ and $A_1^s[n]$ are used in ME/MC to generate two predictions of $A_2[n]$. These two predictions are then combined to generate a final prediction. When we extend this method to two-dimensional wavelet subband, we can shift the original subband horizontally, vertically, and diagonally by 1 pixel to obtain three shifted subbands. We denote these three shifted subbands as LL^h, LL^v, and LL^d. The original subband is denoted as LL^a. Now, instead of having only one reference LL subband, we have four reference LL subbands available at each level for MC. Fig. 4 illustrates the ME/MC block at each level. The design of *combination* block in Fig. 4 remains to be an open problem. In our simulations, we simply took the average of the four predicted subbands. The overall proposed algorithm is described as follows:

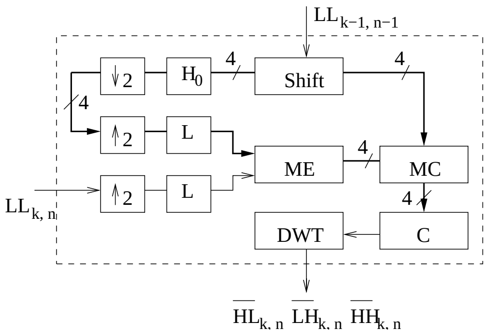

Figure 4: The building block of the proposed ME/MC scheme. C denotes combination of the four predicted subbands.

1. Decompose the current frame I_k into an N level wavelet pyramid.

2. Quantize the subband difference (SD) between $LL_{k-1,N}$ and $LL_{k,N}$ to form the reconstructed lowpass subband $\widetilde{LL}_{k,N}$. Set $n = N$.

3. Apply the ME/MC algorithm described in Fig. 4 to generate three predicted highpass subbands: $\overline{HL}_{k,n}$, $\overline{LH}_{k,n}$, and $\overline{HH}_{k,n}$.

4. Quantize the DSD of the three highpass subbands and form the reconstructed three highpass subbands.

5. Perform wavelet synthesis using $\widetilde{LL}_{k,n}$, $\widetilde{HL}_{k,n}$, $\widetilde{LH}_{k,n}$, and $\widetilde{HH}_{k,n}$ to obtain $\widetilde{LL}_{k,n-1}$.

6. Decrement n by 1. If $n \neq 0$, go back to Step 3.

4. Quantization

In this section, we will discuss the quantization scheme we implemented in encoding the residual subbands. In 4.1, we go through the concept of adpative estimation-quantization. In 4.2, we explain the procedures of quantizer table design in detail.

4.1. Adaptive estimation-quantization framework

For wavelet-based still image coding schemes, zerotree like structure [14, 13] that exploits cross-band correlation is very efficient and successful. But direct application of zerotree structure in our scheme is very difficult, if not impossible. There are two problems that are hard to solve. Firstly, ME/MC are conducted at different levels of wavelet pyramids. This means that the residual subbands at level n are not obtained from filtering and decimating the residual LL_{n-1} subband. So there is not much correlation remains to be exploited between subbands at different levels. Secondly, we must ensure the synchronization in the encoder and the decoder, no information is allowed to be used by encoder if it is not available to the decoder. At each level, both the encoder and the decoder demands availability of reconstructed copy of current frame at the lower resolution (higher level). This requirement implies that we cannot obtain the whole residual pyramid to construct the zerotree hierarchy before quantization. Unlike usual transform based hybrid video coding scheme, in which we conduct ME/MC before quantize the whole frame, here we have a sequence of interleaved operations, *i.e.*, ME/MC→quantization→reconstruction→ME/MC→ quantization→reconstruction→ $\cdots$. To solve this problem, the authors in [11] utilized a predetermined zerotree in the encoder, which is an estimation of the zerotree of the residual pyramid and there is no way to ensure the precision of this estimation. Thus, an ideal quantization scheme for the proposed coding framework must be efficient even if we need to encode subbands individually.

We implement an adaptive context modeling estimation-quantization (EQ) wavelet image coder proposed in [7] to encode each subband in the residual pyramid. In this adaptive EQ coder, wavelet coefficients in each subband are modelled as drawn from an independent generalized Gaussian distribution (GGD) field. Each subband fits into a GGD field of fixed shape, zero mean, and locally slow-varying variances. The probability density function (pdf) of zero-mean GGD is given in [5]:

$$f(x) = \frac{\nu}{2\sigma\Gamma(\nu^{-1})}\sqrt{\frac{\Gamma(3\nu^{-1})}{\Gamma(\nu^{-1})}} \cdot \exp\left(-\left(\sqrt{\frac{\Gamma(3\nu^{-1})}{\Gamma(\nu^{-1})}}\left(\frac{|x|}{\sigma}\right)\right)^{\nu}\right) \quad (2)$$

where σ denotes standard deviation and ν is the shape parameter. For the quantization of each coefficient in the subband, it is assumed that the coefficient concerned and its causal neighbors share identical variance. Thus, a maximum-likelihood estimate of the variance of present coefficient is computed based on causal and quantized neighborhood context. This ensures that the encoder and the decoder keep synchronization because the decoded causal neighbors are available to decoder before the decoding of current coefficient. Once the estimated variance is obtained, it is used to index the entries of a look-up table. Each entry of the table corresponds to a specific quantizer, which is designed off-line according to rate-distortion criterion.

Before proceeding to the design of optimal quantizer, it is necessary to determine which GGD model to use for a given subband. In our scheme, the only parameter we need to specify for the whole subband is the shape parameter ν. We use the kurtosis K of a zero-mean GGD for the purpose of shape-fitting [6]:

$$K = \frac{\langle x^4 \rangle}{(\sigma^2)^2} = \frac{\Gamma(5\nu^{-1})\Gamma(\nu^{-1})}{\Gamma(3\nu^{-1})^2}. \qquad (3)$$

4.2. Optimal quantizer design

An important feature of the EQ coder is that optimal rate-distortion (R-D) quantizers are designed in advance as a function of shape parameters ν, zero-mean ($m = 0$) and unit variance ($\sigma^2 = 1$) and stored as a look-up table. For small ν, the pdf has a sharp peak. The Laplacian density corresponds to $\nu = 1$, while $\nu = 2$ denotes Gaussian density. We used the same shape parameter set as in [5], $\nu \in \{0.5\ 0.6\ 0.7\ 0.8\ 0.9\ 1.0\ 1.5\ 2.0\}$. So, we need to design a set of normalized optimal quantizers for $p(x|m,\sigma,\nu)$, where $m = 0$ and $\sigma = 1$.

We choose to design normalized dead-zone scalar quantizers that are characterized by step size s and dead-zone ratio α. Consider an input random variable X having a pdf of $p(x|0,1,\nu)$, let an n-level dead-zone quantizer $Q^{(n)}(\cdot)$ be defined in terms of its n output values and quantization indices:

$$y_i^{(n)} = \begin{cases} (-\frac{\alpha}{2} + \beta + i - i_0) \cdot s, & 0 \le i < i_0 \\ 0, & i = i_0 \\ (\frac{\alpha}{2} - \beta + i - i_0) \cdot s, & i_0 < i \le n-1 \end{cases} \qquad (4)$$

where i_0 denotes the quantization index of zero bin. In our case, $i_0 = \frac{n-1}{2}$. Because a large number of coefficients having values around zero demands an odd n. β is a real number in the interval [0, 1], which tunes the output value of quantization bins. β has no impact on bit rate, but influences the reconstruction distortion. The quantization index i is determined by:

$$i = \begin{cases} i_0 - \lceil -\frac{x}{s} - \frac{\alpha}{2} \rceil, & x < -\frac{\alpha s}{2} \\ i_0, & -\frac{\alpha s}{2} \le x \le \frac{\alpha s}{2} \\ i_0 + \lceil \frac{x}{s} - \frac{\alpha}{2} \rceil, & x > \frac{\alpha s}{2} \end{cases} \qquad (5)$$

The notation $\lceil \cdot \rceil$ denotes rounding to the next largest integer.

The well-known Lagrangian cost function was employed in the design of the optimal quantizers:

$$J^{(n)} = D^{(n)} + \lambda R^{(n)} \qquad (6)$$

The expected quantizer distortion $D^{(n)}$ is defined by

$$D^{(n)} = \sum_{i=0}^{n-1} \int_{t_{i,low}^{(n)}}^{t_{i,high}^{(n)}} (x - y_i^{(n)})^2 f(x) dx \qquad (7)$$

$t_{i,low}^{(n)}$ and $t_{i,high}^{(n)}$ are the two thresholds that determines the i-th bin. In our dead-zone quantizer, $t_{i,high}^{(n)} - t_{i,low}^{(n)} = s$ when $i \neq i_0$. Based on $t_{i_0,high}^{(n)} = \frac{\alpha s}{2}$, $t_{i_0,low}^{(n)} = -\frac{\alpha s}{2}$, and $t_{i+1,low}^{(n)} = t_{i,high}^{(n)}$, we can recursively determine the thresholds for all bins. The rate is defined by the output entropy of the quantizer:

$$R^{(n)} = -\sum_{i=0}^{n-1} p_i^{(n)} \log_2 p_i^{(n)} \qquad (8)$$

where $p_i^{(n)}$ is the probability of reconstruction value $y_i^{(n)}$,

$$p_i^{(n)} = \int_{t_{i,low}^{(n)}}^{t_{i,high}^{(n)}} f(x) dx \qquad (9)$$

From equations above, it is clear that once λ is fixed, we can always find an optimal solution in the sense of minimizing J by adjusting s, α, and β for an n-level dead-zone scalar quantizer. Since we can obtain an optimal quantizer for any λ, we are able to generate a look-up table that corresponds to a large number of discrete λ values. Note that these quantizers are all normalized to unit variance. In order to quantize a real subband coefficient c with a target λ, we need to use the scaled value $\lambda^\star = \lambda/\hat{\sigma}^2$ as index to the table. $\hat{\sigma}^2$ is the variance estimate of c based on quantized causal neighbors. The stepsize $s_{\lambda^\star}$ of the indexed optimal quantizer needs to be scaled back to $\hat{\sigma} s_{\lambda^\star}$ to quantize c [7]. The symbol probabilities associated with the quantization indices for different GGDs are also pre-stored in a separate table and indexed to be used in arithmetic encoding [16] of the quantization indices.

5. Experimental results

The performance evaluation of the proposed technique is now presented and compared with two other benchmark schemes. The first benchmark scheme is the scheme proposed in [17], in which we used the interpolation filter of length 7 as proposed by the authors. The second scheme is the widely used MPEG-2 codec software [10]. In the experiments we used the luminance component of the full-motion SIF sequence *Football* of size 352×240 at the encoding frame rate of 30 frames/second. The biorthogonal 9/7-tap filter bank [1] was used in DWT. The decomposition level was set to be $N = 3$, which means that the size of the highest level subbands is 44×30. The temporal distance was set to be 1, *i.e.*, ME/MC was done between decomposed reconstructed previous frame $\widetilde{I}_k$ and decomposed current frame I_{k+1}. Also, in order to demonstrate the efficacy of our proposed technique as well as keeping the source coding work as simple as possible, we do not use B frames in our prototype coder. To maintain a fair comparison among the aforementioned three schemes, B frames were also excluded from the MPEG-2 codec. The numer of frames in GOP (group of pictures) was set to 30, *i.e.*, the order of pictures in the encoded bitstream is: $\overbrace{IPP\cdots PP}^{30} I\cdots$

Since the ME/MC is conducted in both encoder and decoder and motion vectors need not to be transmitted, the matching block size in ME/MC is not a problem in the proposed scheme. For a tradeoff between computational complexity and motion vector accuracy, we chose block size of 4×4 for subbands at each level. The search range at Level n is $[-4^{4-n}, +4^{4-n}]$. The motion vectors are computed to full-pel accuracy. To reduce the design complexity of our coder, we did not employ motion compensation to the coarsest resolution (highest level) subband. Instead, we simply quantized the subband difference between $\widetilde{LL}_{k,N}$ and $LL_{k+1,N}$.

Fig. 5 shows the quantized causal neighbors of the current coefficient. Although both 3×3 and 5×5 neighborhood can be used, we have used 3×3 neighborhood in our simulation for simplicity. In the design of optimal normalized quantizer, we choose $n = 65$ as a tradeoff between the reconstruction precision and design complexity. Note that the quantizer table needs to be generated only once and stored as a file. The bin probabilities of each quantizer are also stored as a file. In our simulations, the bitstream rate is controlled by changing λ. It has been found that the output PSNR and rate have marginal fluctuation if we keep the same λ for all frames in one GOP.

Fig. 6 and Fig. 7 demonstrate the efficacy of proposed LBS technique. It has been observed that the proposed technique provides about 2 dB improvement over the benchmark scheme without LBS. The incorporation of LBS technique into backward ME/MC framework boosted the PSNR performance of the reconstructed frames, making the performance comparable to MPEG-2 codec while supporting multi-level scalability. Also, it can be seen from the PSNR

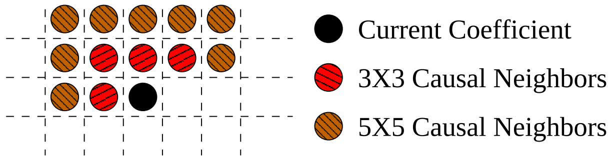

Figure 5: Quantized causal neighborhood of current coefficient.

and bitrate of the first reconstructed frame that the implemented EQ coder is superior to MPEG-2 on encoding I frame. It is necessary to point out that our coding scheme is very primitive, focusing more on the efficacy test of proposed LBS technique. There exists many ways, such as forward/backward ME/MC mode switching, overlapped half-pel MC, joint optimization of ME/MC and residual coding, etc., that can make the codec providing a further improvement in performance..

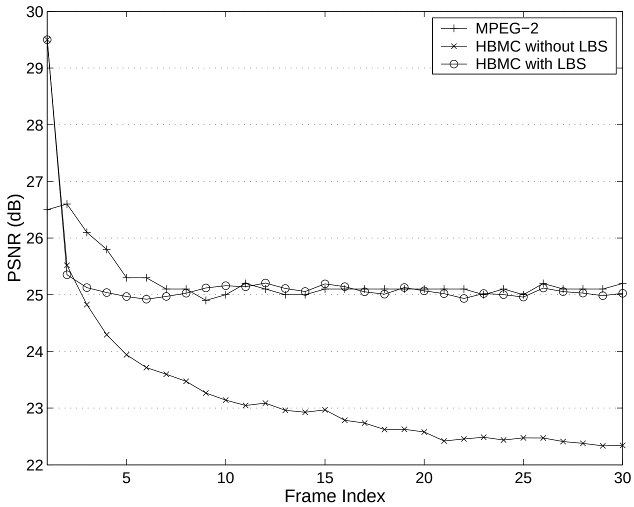

Figure 6: Coding results on SIF sequence *Football*. Comparison of the overall PSNR of the luminance (Y) components at bit rate of 500 Kb/s, 30 frames/s.

6. Conclusions and future work

A multihypothesis hierarchical backward ME/MC framework is proposed in this paper. It is based on the observation that the shifted lowpass subbands in wavelet pyramid of reference video frame can be used in ME/MC scheme to enhance the prediction quality.

For the future work, we are looking into the idea of incorporating forward/backward ME/MC mode switching into current framework to combat the failure of backward ME/MC when complicated motions exist. Fine granularity scalability for the framework will be one interesting topic in further research.

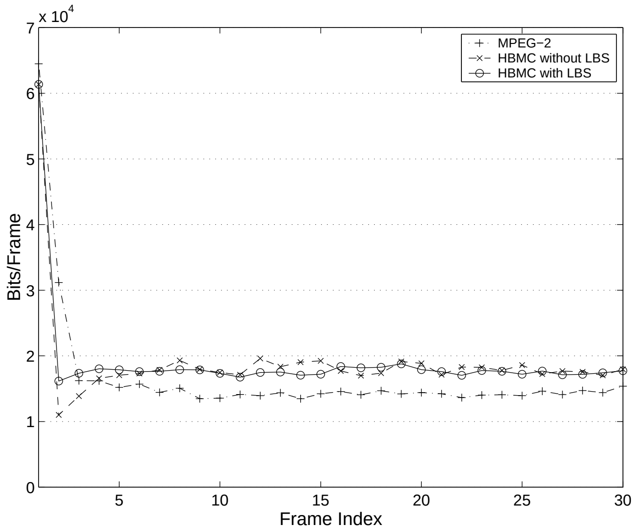

Figure 7: Coding results on SIF sequence *Football*. Comparison of the overall PSNR of the luminance (Y) components at bit rate of 500 Kb/s, 30 frames/s.

7. Acknowledgements

This work was financially supported by the Canadian Space Agency and Canadian Institute for Telecommunication Research (Grant# G119990098). Coding work was based on Fowler's free software package QccPack [3].

References

[1] M. Antonini, M. Barlaud, P. Mathieu, and I. Daubechies. Image coding using wavelet transform. *IEEE Trans. on Image Proc.*, 1(4):205–220, April 1992.

[2] P.-Y. Cheng, J. Li, and C.-C. J. Kuo. Multiscale video compression using wavelet transform and motion compensation. In *Proc. of Inter. Conf. Image Processing*, pages 606–609, 1995.

[3] J. E. Fowler. Qccpack: an open-source software library for quantization, compression, and coding. In *Proc. of IEEE DCC '00*, page 554, 2000.

[4] ISO/IEC JTC 1/SC 29/WG 1. ISO/IEC FCD 15444-1: Information technology — JPEG 2000 image coding system: Core coding system [WG 1 N 1646]. March 2000, http://www.jpeg.org/FCD15444-1.htm.

[5] R. L. Joshi, V. J. Crump, and T. R. Fischer. Image subband coding using arithmetic coded trellis coded quantization. *IEEE Trans. on Circuits and Sys. for Video Tech.*, 5(6):515–523, December 1995.

[6] J. H. Kasner, M. W. Marcellin, and B. R. Hunt. Universal trellis coded quantization. *IEEE Trans. Image Proc.*, 8(12):1677–1687, December 1999.

[7] S. M. LoPresto, K. Ramchandran, and M. T. Orchard. Image coding based on mixture modeling of wavelet coefficients and a fast estimation-quantization framework. In *Proc. of IEEE DCC '97*, pages 221–230, 1997.

[8] A. Lundmark, H. Li, and R. Forchheimer. Motion vector certainty reduces bit rate in backward motion estimation video coding. In *Proc. of SPIE Visual Comm. and Image Processing*, pages 95–104, 2000.

[9] F. G. Meyer, A. Averbuch, and R. R. Coifman. Motion compensation of wavelet coefficients for very low bit rate video coding. In *Proc. of Inter. Conf. Image Processing*, pages 638–641, 1997.

[10] MPEG Software Simulation Group. MPEG-2 Encoder/Decoder. July 1996, ftp://ftp.mpegtv.com/pub/mpeg/mssg/.

[11] A. Nosratinia and M. T. Orchard. A multi-resolution framework for backward motion compensation. In *Proc. of SPIE Electronic Imaging*, pages 190–200, 1995.

[12] H. W. Park and H. S. Kim. Motion estimation using low-band-shift method for wavelet-based moving-picture coding. *IEEE Trans. Image Processing*, 9(4):577–587, April 2000.

[13] A. Said and W. A. Pearlman. A new, fast, and efficient image codec based on set partitioning in hierarchical trees. *IEEE Trans. on Circuits and Sys. for Video Tech.*, 6(3):243–250, June 1996.

[14] J. M. Shapiro. Embedded image coding using zerotrees of wavelet coefficients. *IEEE Trans. on Acoustics, Speech and Signal Proc.*, 41(12):3445–3462, December 1993.

[15] J. Skowronski. Pel-recursive motion estimation and compensation in subbands. *Signal Processing: Image Comm.*, 14:389–396, August 1999.

[16] I. H. Witten, R. M. Neal, and J. G. Cleary. Arithmetic coding for data compression. *Comm. of ACM*, 30(6):520–540, June 1987.

[17] X. Yang and K. Ramchandran. Scalable wavelet video coding using aliasing-reduced hierarchical motion compensation. *IEEE Trans. Image Processing*, 9(5):778–791, May 2000.